B

With this relatively complex system, Boeing obtains a peak current up to about 400 A in pulses of 15 to 20 ps duration, with good emittance. The bunching process yields a peak current which is two orders of magnitude larger than the electron gun current. Space charge forces, which cause the beam to expand both radially and axially, are minimized by using a strong electric field in the high-power buncher, and finally are balanced by forces due to the axial magnetic field. The performance achieved by Boeing appears to be at or near the limit of this type of injector.

Page 8, lines 21-23:

B2

Figure 30 is a schematic drawing of a set of electrode shapes for a high-power diode using the modified formulas to the usual Pierce shapes as discussed below.

Page 11, line 27 through page13, line 4:



A schematic of one embodiment of the proposed device is given in Fig. 2.

Although the design shown is not necessarily optimum it provides a basis for describing the invention. Shown in Fig. 2 is a side view of a cylindrically symmetric device. The rf power is fed into the cavity by a low impedance coaxial transmission line connected to the perimeter of the cavity. Alternatively, rf power may be fed into the cavity by the conventional method of side coupling using a tapered waveguide. The appropriate mode is then set up (in this case the

83

 TM_{020} mode). An annular electron pulse is generated by secondary emission at the second peak of the electric field in the cavity operating in a TM_{020} mode. The first peak is eliminated by placing an inner conducting cylinder at the first zero of the TM_{020} mode. The pulse rapidly bunches and reaches a saturated state within several rf periods. This rapid bunching and saturation is due to a combination of the space charge field and the resonant rf field condition. The right wall of the cavity in Fig. 2 (also see detail) is constructed with a transmitting annular shaped double screen (grid) which allows for the transmission of a high current density hollow electron pulse. The radial wires maintain a path for the rf current. The double screen provides a means to isolate the accelerating and rf fields thus preventing the accelerating field from pulling out electrons that are not resonant with the rf field. Also, the second grid (to the right) is electrically isolated from the first grid and can be dc biased (\approx -100 volts) to create a barrier for low energy electrons. The emittance in the micro-pulse gun (MPG) is lower than would be expected for a dc gun. The main point is that the resonant particles are loaded into the wave at low phase angles and when they reach the opposite electrode or grid, they experience a reduced transverse kick from the grid wires. Inside the cavity, radial expansion is controlled by an axial magnetic field. The short-pulse, high-current electron pulse leaves the cavity with high kinetic energy. The pulse is then accelerated to much higher energy by

-3-

either electrostatic, inductive or rf means. The application for the above hollow beam

configuration is primarily suited to high harmonic microwave production. An alternative

.1

Corold

configuration which produces a solid beam is the TM_{010} mode. This configuration will be more suitable for injector applications.

Page 36, lines 4-23:

D+

In Fig. 17, the "resonant tuning curve" is plotted for the micro-pulse electron gun from the PIC simulations and the theoretical prediction. The importance of this plot is the fact that it describes the "tolerance" of the MPG to deviations in cavity voltage, gap spacing, or frequency, and it indicates the striking agreement between theory and PIC simulation. For simulations with a cavity gap length d = 0.5 cm the peak current density is plotted for various frequencies as a function of the normalized rf field α_0 . Figure 17 suggests that the MPG has a high tolerance, and that errors in the field or gap spacing can be easily accommodated in the resonance process. For instance, as is seen from Table 3 at a frequency of 1.3 GHz, the current density J_x at an applied voltage of 2.4 kV is an order of magnitude less than it is at 4.3 kV. However, J_x climbs rapidly from this value as the voltage approaches 6.4 kV, and then turns over and goes to zero again at 9.8 kV. Also displayed in Fig. 17 is the theoretical tuning curve obtained from the equations above. As can be seen, the agreement between theory and the two-dimensional PIC simulations is excellent. At high $\,\alpha_0^{}$ such that $\,\alpha_0^{}\!>\!0$. 6 the analytic theory is suspect since it does not include relativistic effects.

Page 38, lines 20-25:



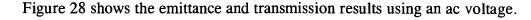
In Fig. 22, the same electric field is shown for the above cavity except a 1 cm diameter, 40 amp/cm², 25 ps long beam is emitted into the cavity. The space charge of the beam decreases the driving electric field by about 1/3. This beam loading, as discussed previously with regard to the tuning curve, does not significantly alter the resonance.

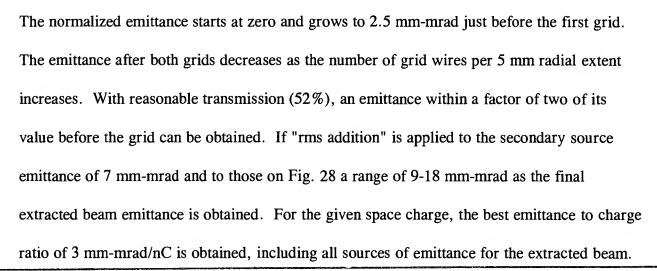
Page 41, lines 3-16:



The accelerating field (after the cavity and second grid) produces a transverse kick as the electrons pass the second grid. However, this field is substantially reduced when we introduce an electrode which makes an angle of 45 ° with the beam exiting the grid. Only the bottom of this 45 ° electrode is shown in Fig. 27. The introduction of this electrode is to focus the micro-pulse; the angle of 45 ° is optional for high energy electrons [W. Peter, Journal of Applied Physics 71, 3197 (1992)]. For emission, this angle becomes $3 \pi/8$, that is, the Pierce angle. The fact that this 45 ° electrode will reduce the transverse fields by an order of magnitude is a fortunate outcome of our studies. This also allows for higher gradients outside the cavity. Thus, the kick from the second grid does not significantly affect the emittance.

Page 42, lines 1-12:





Page 48, lines 1-8:

B8

For the above sample parameters, a 16% expansion occurs. Equation (47) also underestimates the expansion for the same reasons as above so again a numerical integration of the equation of motion was performed. The results show that a 44% expansion of the bunch length occurs, however, the pulse width decreases from 5 psec to about 3.5 psec. These results do not have a significant impact on the performance of the device, as demonstrated in the computer simulations.

Page 48, lines 23 and 24:

where $\lambda = (2e/m)^{1/4}/(9\pi J)^{1/2}$. Integrating this expression gives $\phi(x)$ as a function of x in terms of the following cubic equation

Page 56, lines 8-27:

B0

For a typical injector application, a finite magnetic field at the emitting surface in the MPG is not used because it would impair the emittance downstream. For this reason, an alternative to magnetic focusing within the MPG is proposed, namely to shape the cavity of the MPG so it employs moderate electrostatic focusing. As described above, classical Pierce shaping cannot be directly used in the present situation since the micropulse from the emitter (Fig. 46) is not space-charge limited. In this case, the appropriate electrode shaping can be solved for from the theory presented above. Note that this focusing is essentially "one-way", i.e., the micropulse emitted off the exit grid which returns to the emitting surface S will be slightly de-focused during its transit. However, a slightly de-focused returning pulse can be tolerated since its only raison d'etre is to provide a source of electrons for creation of anew batch of secondary electrons off the surface S. Hence, the only possible disadvantage of a defocused returning micropulse would be to cause some secondary electrons to strike the opposite wall of the cavity outside of S and thus to represent a possible decrease in the cavity O.